Activation mechanism of tantalum niobium flotation by lead ions in a combined collector flotation system

Mingfei He, Shuangke Li, Miao Cao, Yude Gao, Hao Bu, Qingbo Meng

Guangdong Institute of Resources Comprehensive Utilization, Guangzhou 510650, China
State Key Laboratory of Rare Metals Separation and Comprehensive Utilization, Guangzhou 510650, China

Corresponding author: shuangke0215@sina.com (S. Li)

Abstract: The effect of lead ions on the flotation activation of tantalum niobium ore (TNO) was studied by micro-flotation, adsorption capacity experiments, solution chemical composition calculations, and infrared spectral analysis. The experimental demonstrated that the combined collector of salicylhydroxamic acid (SHA) and ammonium dibutyl dithiophosphate (ADDP) resulted in a strong collection capacity for TNO in the presence of lead ions. The solution chemistry calculations determined that the dominant source of lead ions in the aqueous solution was $Pb(OH)^+$ at a pH of 8, which was conducive to the adsorption and interaction of SHA and ADDP anions. In the lead ion activation system, the combined reagent co-adsorbed onto the TNO surface, causing a large negative shift in the zeta potential. The co-adsorption mechanism of the combined collector consisted of complex chemisorption between SHA and the TNO surface active particles, while the main adsorption of ADDP is physisorption.

1. Introduction

Tantalum and niobium are rare metals with high melting and boiling points. They are widely used in numerous industries, such as aerospace and electronic energy, superconducting, biomedical engineering, and special steel industries, due to their corrosion resistance, superconductivity, unipolar conductivity, high strength at high temperatures, and their production of suction (Iborra-Torres et al., 2020; Izawa and Nomura, 2020; Rodrigues et al., 2020; Unkrig et al., 2020). They have been employed in various materials, including electronics, precision ceramics, electro acousto-optic devices, and cemented carbide (Nanda et al., 2020; Song et al., 2020; Xiao et al., 2020; Zheng et al., 2020). Presently, the separation technology for purifying tantalum niobium ore (TNO) in foreign countries mainly adopts the gravity separation method. Flotation separation is used to recover tailings or fine-grained materials from this separation method (Deblonde et al., 2016; Liu et al., 2016; Purcell et al., 2018). However, the nature of domestic ore is complex, which needs to be treated in combination with gravity, magnetism, electricity, flotation, and metallurgy purification processes. Although the flotation method does not play a leading role in the separation process of TNO, it has a significant recovery effect on tantalum, niobium, tungsten, and tin ores with similar physical properties (Li et al., 2019; Liu et al., 2020; Thi Hong and Lee, 2019).

Tantalum niobium slime is not an ore, but it is the primary component for improving TNO recovery. Generally, gravity separation has a negligible effect on the recovery of fine-grained materials. Yuan et al. (2015) treated micro-fine TNOs from Songzi using the following process: classification, gravity concentration, magnetic separation, middling regrinding, and another gravity concentration. They obtained Ta_2O_5 and Nb_2O_5 with grades of 7.03% and 3.54% and recoveries of 49.42% and 35.46% respectively. Researchers have extensively studied flotation reagents for processing TNO. The common

collectors of tantalum and niobium are fatty acids, arsenic acids, phosphonic acids, hydroxamic acids, and cationic collectors. Among them, collectors with -COOH, -SO_4H, and -SO_3H functional groups exhibit strong collection ability but poor selectivity. Hydroxamic acids have low toxicity and good selection, but they require large dosages; phosphonic acids are strong collectors, but are sensitive to Fe^{2+} and Ca^{2+} ions and have mild toxicity; and arsenic acids have strong collection abilities, good selectivities, but high toxicity (Huang et al., 2020; Xiao et al., 2019a; Xiao et al., 2019b). Ji et al. (2004) analyzed the crystal structure of niobate rutile in Baiyunebo ore, as well as its infrared spectra before and after the interaction between niobate rutile and alkylhydroxamate within the ore. Their results showed that the niobate rutile and alkylhydroxamate both exhibit chemisorption, and the active particles (Nb^{5+}, Fe^{3+}, and Ti^{4+}) on the niobate rutile surface combined with hydroxamate ions from alkylhydroxamate to form a stable, pentahydrate, meta-chelating ring. Compared with fatty acids, hydroxamic acids have a weaker ability to collect fine tantalum and niobium. This can be ascribed to their higher solubility with compounds formed by cations on the mineral surface, and its lower adsorption stability on the mineral, and its easy desorption from the mineral surface (Lv et al., 2017). Furthermore, the larger dosage of hydroxamic acid increases the beneficiation cost, so combining collector is a widely used strategy in flotation of oxdized minerals. Therefore, it is necessary to further investigate the flotation of TNO with modified fatty acids and combined collectors, and to explore the effect on recovering TNO. Salicylhydroxamic acid (SHA) is another hydroxamic acid flotation collector, which can form stable chelates with tungsten, tin, tantalum, niobium, and other metal oxides. Since a small amount of sulfide collectors, such as xanthate, can improve the production index when hydroxamic acid collectors are used, this paper attempts to explore the flotation behavior of sulfide collectors for oxidized ore.

In particular, there is little research on the auxiliary collector ammonium dibutyl dithiophosphate (ADDP), which is commonly employed in the flotation of oxidized ore. Therefore, this paper also reports on the effects of lead ions on the activation mechanism of TNO when a combination of ADDP and SHA is applied. The results of this study provide insight for developing flotation theory of fine-grained TNO.

2.   Materials and methods

2.1. Materials and reagents

Tantalum niobium ore (TNO) was obtained from a gravity concentration tantalum niobium concentrate of Ethiopian. After the samples were separated by graded magnetic separation, the ceramic ball mill was used to dry grind the samples until the particle size was less than 0.074 mm. Then, the deionized water was used for repeated cleaning and then dried in a vacuum drying oven for subsequent tests. The chemical compositions of TNO were determined by a wavelength dispersive X-ray fluorescence (XRF) using S4 Pioneer spectrometer (PANalytical B.V., Almelo, The Netherlands). The results of XRF are shown in Table 1. The results demonstrated that the purity of TNO in the sample were calculated to be 90.25%. Sulphuric acid and sodium hydroxide of analytically pure grade were obtained from Sinopharm Chemical Reagent Co., Ltd. Salicylhydroxamic acid (SHA) and ammonium dibutyl dithiophosphate (ADDP) with industrial grade were purchased obtained from Zhuzhou Flotation Reagents. Ultra-pure water with a conductivity of 18.2 MΩ·cm was obtained from a USF-ELGA Maxima water purification system.

Table 1. The results of chemical composition analysis of mineral samples (wt.%)

Sample	Ta_2O_5	Nb_2O_5	FeO	MnO	Li_2O	Other
TNO	39.12	35.46	8.21	7.36	0.21	9.64

2.2. Micro-flotation tests

The single mineral flotation test was carried out in a 40 ml XRF Ⅱ aerated hanging cell flotation machine with a fixed rotating speed of 1992 r/min. The test steps were as follows: firstly, added 2.00 g single mineral and a certain amount of ultrapure water into the flotation cell. After stirring for 1 min, used HCl or NaOH to adjust the pH of the solution to the specified value, and continue stirring for 2 min. According to the needs of the test, a certain amount of activator was added, acting for 3 min; and then

the combined collectors were added in sequence of SHA and ADDP, stirring for 3 min respectively. Finally, after adding proper amount of foaming agent, the pulp volume was fixed to 40 ml, and stirred for 1min. Before flotation, the pH value of pulp was measured, and then the flotation was started by hand scraping. The flotation time was 3 min. The concentrates and tailings were weighed after filtration and drying, and the flotation recovery was then calculated.

2.3. Zeta potential measurements

The zeta potential of TNO surface was measured using a ZetaPALS instrument (Brookhaven, MS, USA). The samples were ground to less than 5 μm. The suspension was prepared by adding 20 mg of TNO to 5 mL of distilled, deionized water containing 10^{-3} mol/L KCl as a supporting electrolyte. The resulting suspension was conditioned for 15 min during which suspension pH was measured. The pH was adjusted using either NaOH or H_2SO_4 over a pH range of 2–12. The reported results were the average of at least three full repeats of the experiments.

2.4. Adsorption amount measurements

The treatment time and order of addition of the reagents were the same as micro-flotation tests, except that the flotation was not carried out. The suspension was agitated for 5 min. After each step of the extraction process the samples were centrifuged and filtered to separate the liquid and solid phases. After washing twice with deionized water, the filter liquor was moved to a 100-mL volumetric flask. The adsorption amount was calculated by Equation (1):

$$Q_e = \frac{V(C_0 - C_e)}{100m} \tag{1}$$

where, Q_e is the mount of Pb^{2+} ions or collectors adsorbed on the TNO surface (mg/g); C_0 and C_e is the initial and residual concentration of Pb^{2+} ions or collectors (mg/L), respectively; V is the volume (L); m is the mass of TNO (g).

2.5. FT-IR analysis

The SHIMADZU IR Affinity-IS Fourier transform infrared spectrometer were carried out with a KBr disk that contained 0.5% of the required sample to scan in the wave number range of 4000 to 500 cm^{-1} at a resolution of 4 cm^{-1}. To prepare the samples for FT-IR analysis, the Pb^{2+} ions, SHA and ADDP were 20 times the dosage which were respectively added in the micro-flotation process, and the time and order for them adding was same to the micro-flotation. Finally, the solid samples were washed three times using deionized water with the same pH and allowed to dry at the room temperature to FT-IR analyses.

3.   Results and discussion

3.1. Micro-flotation tests

The effects of pulp pH and collector dosage on the flotation recovery of TNO were investigated (Fig. 1). Fig. 1a showed that when the concentration of SHA was 800 mg/L, the flotation recovery of TNO initially increased and then decreased with an increasing pH (Fig. 1a). When the pH was 8, a maximum flotation recovery of 70% was achieved. However, when ADDP was used as the flotation collector, the flotation recovery of TNO was less than 20% and did not fluctuate at the whole pH range.

The relationship between the flotation recovery of TNO and the dosage of collector was determined (Fig. 1b). We found that when the pH was 8.0, the flotation recovery of TNO increased with an increase in SHA concentrations, and when the dosage of SHA was 1000 mg/L, the flotation recovery of TNO reached 82% and was relatively stable. A similar trend was observed as the concentration of ADDP was increased, where the flotation recovery of TNO slowly increased. However, a recovery more than 20% was never achieved, which indicated that the collection capacity of butylamine was very poor for TNO, and that it was not suitable as a flotation collector for TNO when it was along used.

In general, the Pb^{2+} ion has a good activation effect on oxidized ore; therefore, its effects on the flotation recovery of TNO under various conditions were tested (Fig. 2). When the concentration of SHA was 200 mg/L, the flotation recovery of TNO first increased and then decreased as the pH continued to

rise (Fig. 2a). The maximum flotation recovery of 71.62% was obtained when the pH was 8.0. Similarly, when ADDP was used as the collector, the recovery of initially increased and then decreased with the increase in pH; the maximum flotation recovery of 41.36% was achieved when the pH was 7.9. Compared with Fig. 1a, it was found that when lead ions were present, the amount of collector was greatly reduced, indicating that the activation effect of the lead ions on tantalum niobium flotation was indisputable.

Fig. 1. The effect of pH (a) and dosage of collector (b) on the flotation recoveries of TNO. a - C[SHA] = 800 mg/L, C[ADDP] = 1000 mg/L, C[MIBC] = 20 mg/L, b - pH=8.0

When the pH of the pulp was 8, the flotation recovery of TNO gradually increased with collector concentration until it stabilized (Fig. 2b). When the dosage of SHA was 350 mg/L, the flotation recovery reached 90%, and when the amount of ADDP was 180 mg/L, the recovery was 48%. The flotation recovery of TNO first increased with the increase in Pb^{2+} concentration, and then it stabilized (Fig. 2c). When the concentration of lead nitrate reached 40 mg/L in the SHA flotation system, the TNO flotation recovery reached a stable value of proximately 75%. In the activation system with 100 mg/L of ADDP, the TNO recovery increased with the increase in Pb^{2+} concentration and when the concentration of Pb^{2+} was 60 mg/L, the recovery of TNO was 42%.
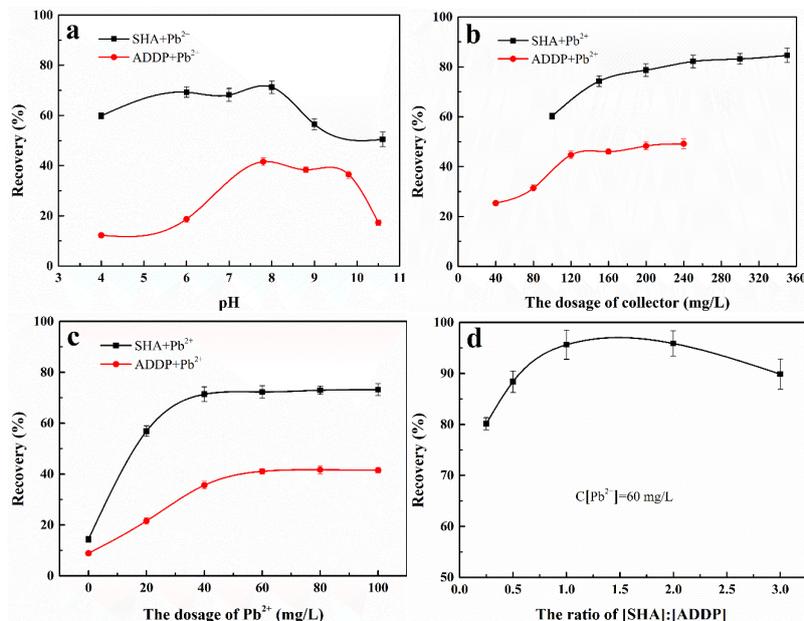

Fig. 2. After activation of Pb^{2+} ions，the effects of pH(a), dosage of collect (b), dosage of Pb^{2+} (c) and ratio of C[SHA]:C[ADDP] on the recovery of TNO. a - C[SHA] = 200mg/L, C[ADDP] = 100 mg/L, C[Pb^{2+}] = 6 0mg/L, C[MIBC] = 20 mg/L, b - pH = 8.0; C[Pb^{2+}] = 60 mg/L, C[MIBC] = 20 mg/L, c - pH = 8.0, C[SHA] = 200 mg/L, C[ADDP] = 100mg/L, C[MIBC] = 20 mg/L, d - pH = 8, C[Pb^{2+}] = 60 mg/L, C[SHA]+C[ADDP] = 200 mg/L, C[MIBC] = 20 mg/L

When the ratio of SHA concentration to ADDP concentration increased, the TNO recovery initially increased as well and then decreased (Fig. 2d). When the concentration ratio of SHA to ADDP was 1:1, the recovery of tantalum niobium flotation was 95.5%. These results suggested that combining SHA and ADDP in a 1:1 ratio improved the collection ability for TNO.

3.2. Adsorption amount measurements of flotation reagents on the TNO surface

To elucidate the relationship between the adsorption behavior of flotation reagents on the mineral surface and the flotation recovery, the relationship between the adsorption capacity of flotation reagents on the TNO surface and the pH value was studied (Fig. 3).

When the solution pH was in the range of 7-10, the adsorption capacity of Pb^{2+} ions on the TNO surface was more than 95% in the absence of collector (Fig. 3a). When there were collectors present in the system, the adsorption capacity of Pb^{2+} onto the mineral surface decreased to some extent, indicating that the collectors had selective dissolution effect on the lead ions that had be adsorbed on the TNO surface. As for the difference in the adsorption capacity of Pb^{2+}, it could be caused by differences in adsorption modes. The adsorption capacity of SHA and ADDP on the TNO surface was observed to clearly increase after the addition of lead ions, and the adsorption capacity curve was in good agreement with the recovery curve of single mineral flotation tests of TNO (Fig. 3b).

The relationship between the pH and the adsorption capacity of the combined collector on the TNO surface was analyzed (Fig. 3c), where a lead ion concentration of 1.8×10^{-4} mol/L, SHA concentration of 3.92×10^{-4} mol/L, and ADDP concentration of 2.32×10^{-4} mol/L. The comparison between Fig. 3b and Fig. 3c indicated that the adsorption capacity of SHA and ADDP in the combined collector system was slightly higher than of the single collector systems, which could be ascribed to the synergistic effect between SHA and ADDP.
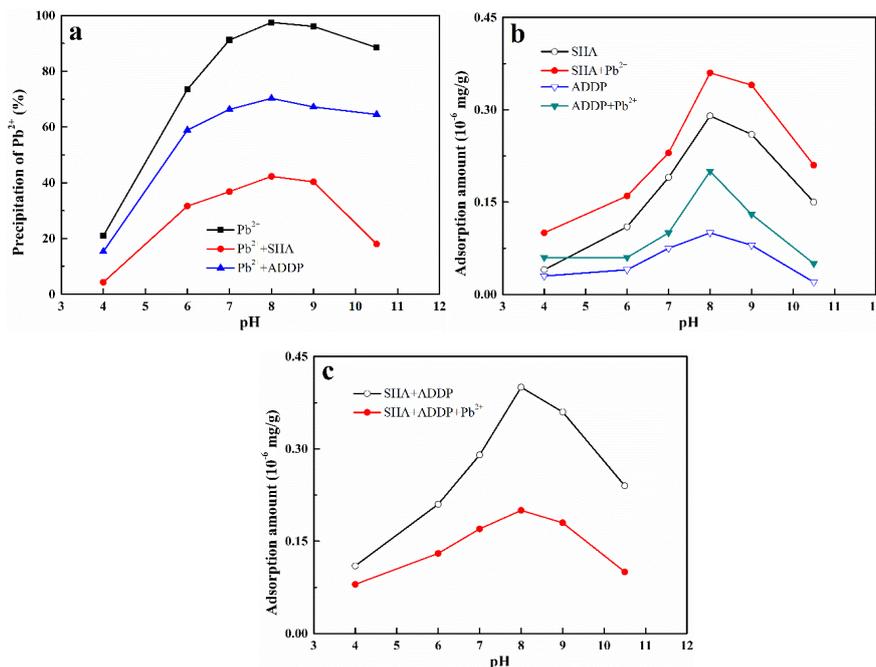

Fig. 3. Adsorption amount of flotation reagents on the TNO surface as a function of pH. a - Pb^{2+} ions, b - single collector, c - combined collector. $C[Pb^{2+}] = 1.8\times10^{-4}$ mol/L, $C[SHA] = 3.92\times10^{-4}$ mol/L, $C[ADDP] = 2.32\times10^{-4}$ mol/L

3.3. Calculation of chemical composition of reagents

The lead component plays a key role in the flotation of TNO, so it is of great theoretical significance to study the existence form and physicochemical properties of lead nitrate in aqueous solutions and at the TNO/water interface. In general, metal ions in aqueous solutions are ionized and hydrolyzed to produce homogeneous precipitates, or they react with collectors to form complexes or other precipitates

(Xiao et al., 2018; Xiao et al., 2017). At the mineral/water interface, metal ions or their hydroxides precipitate and bond with the mineral lattice, adsorbing onto the mineral surface. Lead ions are hydrolyzed in aqueous solution, and their forms vary greatly under different pH conditions. Through the chemical composition calculations of the solution, the concentrations of various lead components at different pH values can be determined.

The initial concentration of lead ion was set to 1.8×10^{-4} mol/L, and calculated the logarithm of each component concentration of lead ion in the effluent solution as shown in Fig. 4a.

The initial SHA concentration was set to 3.92×10^{-4} mol/L, and the logarithm diagram of each subsequent concentration of SHA in the solution was calculated (Fig. 4b). The hydroxyl groups in SHA molecules connected with nitrogen atoms are easy to ionize hydrogen ions, making it weak acidic. With the change of pH value, the ionization equilibrium of hydrogen ions will change accordingly.

When the pH of the solution was less than 7.4, the dominant component in the solution was SHA, and when it was greater than 7.4, the dominant component in the solution was the SHA anion. When the solution pH was greater than 9, the concentration of OH$^-$ in the solution gradually increased, which resulted in competitive adsorption between the hydroxide ion and the SHA anion. This results in a reduced flotation recovery rate for the lead ion/SHA system. Furthermore, when the solution pH was equal to its *pKa* value, the molecular concentration of the SHA anion and SHA in the solution were the same, resulting in the easy formation of a molecular association complex that could co-adsorb onto the mineral surface.
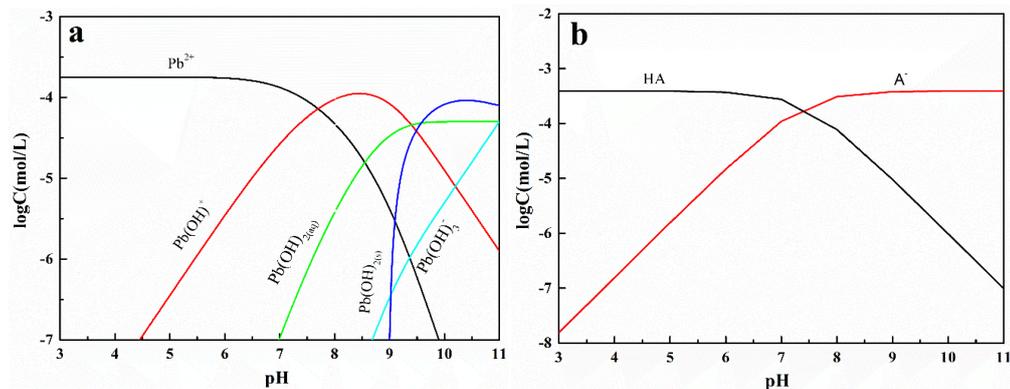
Fig. 4. The chemical composition of Pb^{2+} ions (a) and SHA (b) as a function of pH value

3.4. Zeta potential measurements

The adsorption of cations or anions onto a mineral inevitably leads to a change in the surface charge. The potential relationship between the pulp pH and the TNO surface after the chemical reaction of the activation system was studied (Fig. 5). Fig. 5a showed that the isoelectric point (IEP) of TNO in ultrapure water was 3.5. After adding 50 mg/L of lead ions, the zeta potential curve moved an overall positive shift, and IEP increased to 3.9. In the activation system, when SHA and ADDP were both added, the zeta potential curve shifted in a negative direction, indicating that the collector anions adsorbed onto the TNO surface. When the pH was less than 7.5, the negative shift of the curve of ADDP was greater than that of SHA. This could be because that the dominant component of ADDP in this pH range was the ADDP anion, while that of SHA was mainly its molecular form (Fig. 4b). When the solution pH was greater than 7.5, the negative shift of the curve of SHA was greater than that of ADDP, because the dominant component of SHA began to convert an anion in this pH range. All the lead components in the solution may adsorb onto the TNO surface. In fact, when the pH was less than 7.5, the dominant component of lead in the solution was Pb^{2+}, whose adsorption onto the TNO surface resulted in a increase in the surface zeta potential (Fig. 4a). With the increase in pH, Pb(OH)$^+$ gradually became the dominant component in solution. Since Pb(OH)$^+$ has very high activity and it easily chemisorbs onto the TNO surface, which covers the surface with more positive ions and causes the zeta potential to shift in a positive direction. When the solution pH increased to 9.01, the lead ions began to form hydroxide precipitates, and as the pH value continued to increase above 11, Pb(OH)$_3^-$ gradually *became* the

dominant component in the system. This compound had difficultly adsorbing onto the TNO surface. Therefore, it has litter effect on the surface potential of TNO.

The zeta potential diagram of the TNO surface after the activation system is affected by the pulp pH and the combined collector, where the collector concentration was found to be half that the value when a single collector was used (Fig. 4b). After adding the combined collector, the zeta potential curve on the TNO surface showed an overall negative shift, indicating the adsorption of the combined collector onto the TNO surface. When the total amount of collectors was constant, the negative zeta potential shift of the TNO surface by the combined collector was larger than that caused by two single collectors, which indicated that the adsorption effect on the mineral surface was superior to that of the two single collectors.
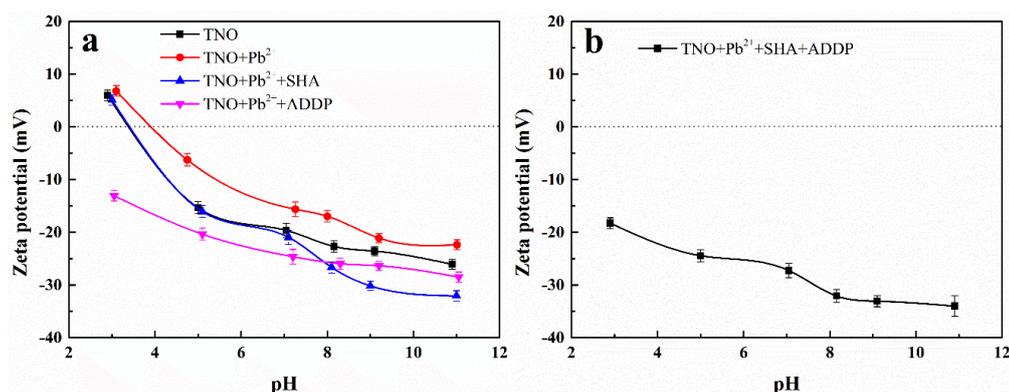

Fig. 5. Zeta potential of the TNO surface before and after reagent treatment. a - $C[Pb^{2+}]$ = 50 mg/L, C[SHA] = 200 mg/L, C[ADDP] = 200 mg/L, b - $C[Pb^{2+}]$ = 50 mg/L, C[SHA] = 100 mg/L, C[SHA] = 100 mg/L

3.5. FT-IR analysis

Infrared light causes, the functional groups or chemical bonds of organic molecules to vibrate and absorb the light. Different functional groups or chemical bonds display different absorption frequencies for infrared light, and changes in their positions are reflected in their infrared spectrum. By comparing the infrared spectra of SHA and ADDP before and after their interaction with TNO (Fig. 6), information regarding changes in their chemical bonds or functional groups can be observed.

Fig. 6a showed the infrared spectrum of SHA before and after its interaction with the Pb^{2+} ions. The characteristic band of SHA was located at 3289 cm^{-1} corresponds to the superposition of the O-H and N-H stretching vibrations (Meng et al., 2020). At 3116 cm^{-1} and 1618 cm^{-1}, the stretching vibrations of N-H and C=O, respectively, could be found (Xiong et al., 2020). The bands at 1524.18 cm^{-1} and 1489 cm^{-1} represented the benzene ring C=C stretching vibrations; those at 1247 cm^{-1} and 1101 cm^{-1} correspond to the benzene ring C-N stretching vibration; and the bands at 906 cm^{-1}, 744 cm^{-1}, and 620 cm^{-1} indicated the benzene ring C-H out-of-plane deformation vibrations. After the reaction between SHA and Pb^{2+} ions, the characteristic band of SHA shifted from 3289 cm^{-1} to 3443 cm^{-1}; the C=O band shifted from 1618 cm^{-1} to 1383 cm^{-1}; the C-N stretching vibration band and the C-H bending vibration band of the benzene ring also shifted (Meng et al., 2020). Although no new absorption peaks were found, the observed shifts indicated that when SHA acted on the TNO surface in the activation system, the Pb^{2+} ions may be acting as the active adsorption particles (Zhao et al., 2020).

Fig. 6b showed the infrared spectrum of ADDP before and after its interaction with the Pb^{2+} ions. At 3167 cm^{-1} the stretching vibration band of the N-H bond, while those at 2960 cm^{-1}, 2805 cm^{-1}, and 1466 cm^{-1} represented the antisymmetric stretching, symmetric stretching, and antisymmetric deformation vibration bands, respectively, of the -CH$_3$ moiety (Zhang and Qin, 2015; Zhang et al., 2014). The band at 1397 cm^{-1} corresponded to the bending vibration of N-H; that at 993 cm^{-1} was the stretching vibration band of the P-O-C bond; and the bands at 664 cm^{-1} and 564 cm^{-1} represented the strong and weak absorption bands, respectively, of the P-S$_2$ stretching. Similarly, to that of SHA, there were no new absorption peaks observed after the reaction between ADDP and the Pb^{2+} ions, but small shifts of several characteristic ADDP peaks indicated that when ADDP acted on the TNO surface in the activation system, the lead ions may act as the active particles for adsorption.

Furthermore, the infrared spectrum of tantalum niobium before and after interaction with Pb^{2+} ions were obtained (Fig. 6c), where the bands at 837 cm^{-1}, 706 cm^{-1}, and 646 cm^{-1} were all characteristic peaks of TNO. After Pb^{2+} ion treatment, the characteristic peaks of the infrared spectrum remained unchanged, which indicated a lack of chemisorption between the Pb^{2+} ions and the TNO surface.

The interactions of TNO with a single reagent and a combined reagent under the activation system were monitored via infrared spectrum as well (Fig. 6d). The results suggested that there were no obvious changes in the absorption band of the TNO surface with only ADDP present, which indicated that there was no chemisorption of the ADDP onto the TNO surface under the activation system. However, small shifts in the characteristic SHA bands were observed after its interaction with TNO. The stretching vibration of the C=O moiety in the SHA molecule appeared at 1580 cm^{-1}; the stretching vibration of the C=C bonds in the benzene ring appeared at 1490 cm^{-1} and 1370 cm^{-1}; and the stretching vibrations of C-N bond in SHA appeared at 1240 cm^{-1} and 1140 cm^{-1}. These results indicated that there was chemisorption of the hydroxamic acid onto the surface of TNO in the activated system, and it was speculated that there may be multiple-ring chelates forming between the hydroxamic acid and Mn^{2+} particles on the TNO surface, according to the molecular structure. The absorption peak of the combined reagents was similar to that of the activated system with only SHA. However, the characteristic peak of the former was stronger than that of the latter, indicating that SHA was chemically adsorbed onto the TNO surface when the combining reagents were used, while ADDP primarily acted on the mineral surface through physisorption.

Based on the experimental results of the present study, we construct a model for the adsorption of Pb^{2+} and SHA on the TNO surface. Fig. 7 showed a schematic illustration of the adsorption model. When Pb^{2+} and SHA were added to the TNO suspension, the lead species either adsorbed on the TNO surface, increasing the number of active sites.
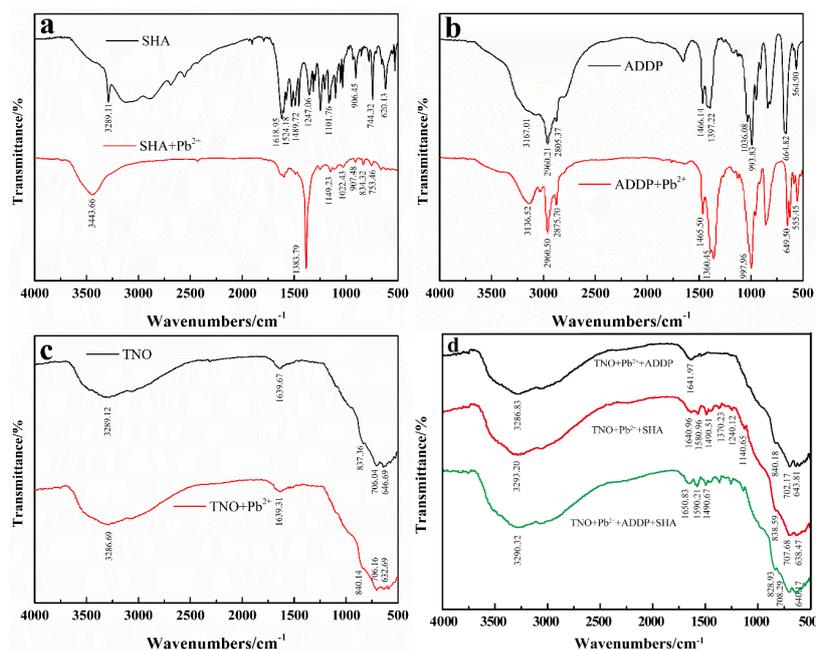

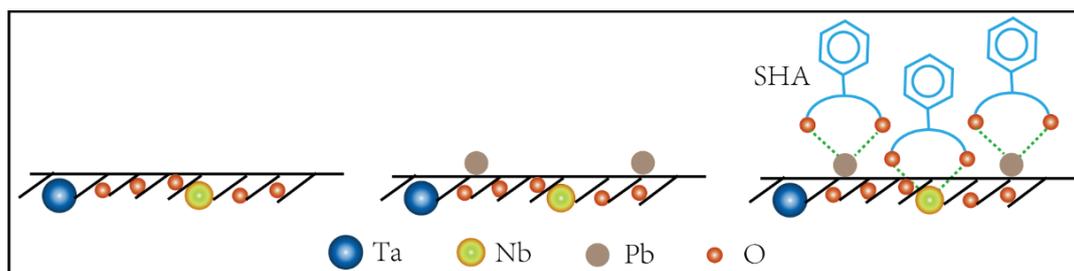Fig. 6. FT-IR of reagents and TNO before and after treatment

Fig. 7. Schematic illustration of the adsorption model for Pb^{2+} and SHA on the TNO surface

4. Conclusions

In summary, we investigated the effects of Pb^{2+} ions on the flotation behavior of TNO with SHA and ADDP as a combined collector and revealed the interaction mechanism between these flotation reagents and the TNO surface.

When SHA and ADDP were combined in a 1:1 ratio, the flotation recovery of TNO reached 96.23%. Furthermore, the SHA and ADDP combined collector adsorbed onto the TNO surface, resulting in a large negative shift in the zeta potential. The adsorption mechanism of the combined collector was proposed to involve complex chemisorption between SHA and TNO surface active particles, while the ADDP primarily acted on the mineral surface via physical adsorption.

Acknowledgments

References

DEBLONDE, G.J.P., WEIGEL, V., BELLIER, Q., HOUDARD, R., DELVALLEE, F., BELAIR, S., BELTRAMI, D., 2016. *Selective recovery of niobium and tantalum from low-grade concentrates using a simple and fluoride-free process*. Separation and Purification Technology 162, 180-187.

HUANG, X., ZHU, T., DUAN, W., LIANG, S., LI, G., XIAO, W., 2020. *Comparative studies on catalytic mechanisms for natural chalcopyrite-induced Fenton oxidation: Effect of chalcopyrite type*. Journal of Hazardous Materials 381, 120998.

IBORRA-TORRES, A., KULAK, A.N., PALGRAVE, R.G., HYETT, G., 2020. *Demonstration of Visible Light-Activated Photocatalytic Self-Cleaning by Thin Films of Perovskite Tantalum and Niobium Oxynitrides*. ACS applied materials & interfaces 12, 33603-33612.

IZAWA, I., NOMURA, K., 2020. *(Arylimido)niobium(V)-Alkylidenes, Nb(CHSiMe₃)(NAr) OC(CF₃)₍₃₎ (PMe₃)₍₂₎, That Enable to Proceed Living Metathesis Polymerization of Internal Alkynes*. Macromolecules 53, 5266-5279.

JI, J., 2004. *Study on the reaction mechanism between ilmenorutile and alkylhydroxyoxime*. Nonferrous Metals 4, 42-44.

LI, J., LI, P., WANG, D., LI, X., 2019. *A review of niobium and tantalum metallogenic regularity in China*. Chinese Science Bulletin-Chinese 64, 1545-1566.

LIU, M., YOU, Z., PENG, Z., LI, X., LI, G., 2016. *Enrichment of rare earth and niobium from a REE-Nb-Fe associated ore via reductive roasting followed by magnetic separation*. JOM 68, 567-576.

LIU, Z., XIU, T., DU, Y., WANG, Y., 2020. *Leaching characteristics and kinetics of radioactive element uranium and thorium from Ta/Nb tailing*. Journal of Radioanalytical and Nuclear Chemistry 323, 1197-1206.

LV, J., ZHANG, H., TONG, X., FAN, C., YANG, W., ZHENG, Y., 2017. *Innovative methodology for recovering titanium and chromium from a raw ilmenite concentrate by magnetic separation after modifying magnetic properties*. Journal of Hazardous Materials 325, 251-260.

MENG, Q., YUAN, Z., LI, L., LU, J., YANG, J., 2020. *Modification mechanism of lead ions and its response to wolframite flotation using salicylhydroxamic acid*. Powder Technology 366, 477-487.

NANDA, G., AWIN, E.W., GASYAK, T., KOROLEVA, E., FILIMONOV, A., VAKHRUSHEV, S., SUJITH, R., KUMAR, R., 2020. *Temperature dependent conductivity and broadband dielectric response of precursor-derived Nb₂O₅*. Ceramics International 46, 9512-9518.

PURCELL, W., POTGIETER, H., NETE, M., MNCULWANE, H., 2018. *Possible methodology for niobium, tantalum and scandium separation in ferrocolumbite*. Minerals Engineering 119, 57-66.

RODRIGUES, L.M., LIMA ZUTIN, E.A., SARTORI, E.M., MENDONCA, D.B.S., MENDONCA, G., CARVALHO, Y.R., *Reis de Vasconcellos, L.M., 2020. Influence of Titanium Alloy Scaffolds on Enzymatic Defense against Oxidative Stress and Bone Marrow Cell Differentiation*. International journal of biomaterials 2020, 1708214-1708214.

SONG, T., TANG, H.P., LI, Y., QIAN, M., 2020. *Liquid metal dealloying of titanium-tantalum (Ti-Ta) alloy to fabricate ultrafine Ta ligament structures: A comparative study in molten copper (Cu) and Cu-based alloys*. Corrosion Science 169, 108600.

THI HONG, N., LEE, M.S., 2019. *A review on the separation of niobium and tantalum by solvent extraction*. Mineral Processing and Extractive Metallurgy Review 40, 265-277.

UNKRIG, W., ZHE, F., TAMIM, R., OESTEN, F., KRATZERT, D., KROSSING, I., 2020. Cationic Niobium-Sandwich and Piano-Stool Complexes. Chemistry (Weinheim an der Bergstrasse, Germany). DOI:10.1002/

chem.202003748.

XIAO, L., XU, X., LIU, S., SHEN, Z., HUANG, S., LIU, W., PENG, Y., HUANG, Y., LIU, J., NIE, Y., ZHAO, X., CAI, Z., 2020. *Oxidation behaviour and microstructure of a dense MoSi2 ceramic coating on Ta substrate prepared using a novel two-step process*. Journal of the European Ceramic Society 40, 3555-3561.

XIAO, W., CAO, P., LIANG, Q., HUANG, X., LI, K., ZHANG, Y., QIN, W., QIU, G., WANG, J., 2018. *Adsorption behavior and mechanism of Bi(III) ions on rutile-water interface in the presence of nonyl hydroxamic acid*. Transactions of Nonferrous Metals Society of China 28, 348-355.

XIAO, W., CAO, P., LIANG, Q., PENG, H., ZHAO, H., QIN, W., QIU, G., WANG, J., 2017. *The Activation Mechanism of Bi^{3+} Ions to Rutile Flotation in a Strong Acidic Environment*. Minerals 7, 113.

XIAO, W., REN, Y., YANG, J., CAO, P., WANG, J., QIN, W., QIU, G., 2019a. *Adsorption mechanism of sodium oleate and styryl phosphonic acid on rutile and amphibole surfaces*. Transactions of Nonferrous Metals Society of China 29, 1939-1947.

XIAO, W., ZHAO, Y., YANG, J., REN, Y., YANG, W., HUANG, X., ZHANG, L., 2019b. *Effect of sodium oleate on the adsorption morphology and mechanism of nanobubbles on the mica surface*. Langmuir 35, 9239-9245.

XIONG, W., DENG, J., ZHAO, K., WANG, W., WANG, Y., WEI, D., 2020. *Bastnaesite, barite, and calcite flotation behaviors with salicylhydroxamic acid as the collector*. Minerals 10, 282.

YUAN, Z., LU, J., WU, H., LIU, J., 2015. *Mineralogical characterization and comprehensive utilization of micro-fine tantalum–niobium ores from Songzi*. Rare Metals 34, 282-290.

ZHANG, T., QIN, W., 2015. *Floc flotation of jamesonite fines in aqueous suspensions induced by ammonium dibutyl dithiophosphate*. Journal of Central South University 22, 1232-1240.

ZHANG, T., QIN, W., YANG, C., HUANG, S., 2014. *Floc flotation of marmatite fines in aqueous suspensions induced by butyl xanthate and ammonium dibutyl dithiophosphate*. Transactions of Nonferrous Metals Society of China 24, 1578-1586.

ZHAO, W., LIU, D., FENG, Q., 2020. *Enhancement of salicylhydroxamic acid adsorption by Pb(II) modified hemimorphite surfaces and its effect on floatability*. Minerals Engineering 152, 106373.

ZHENG, Q., WU, F., CHEN, L., QIAN, F., YANG, K., GE, Z., SONG, P., FENG, J., 2020. *Thermophysical and mechanical properties of YTaO$_4$ ceramic by niobium substitution tantalum*. Materials Letters 268.